

A Continuum Description of Vibrated Sand

Jens Eggers* and Hermann Riecke†

* *Universität Gesamthochschule Essen, Fachbereich Physik, 45117 Essen, Germany*

† *Department of Engineering Sciences and Applied Mathematics, Northwestern University, Evanston, Illinois, 60208, USA*

The motion of a thin layer of granular material on a plate undergoing sinusoidal vibrations is considered. We develop equations of motion for the local thickness and the horizontal velocity of the layer, where the driving comes from the violent impact of the grains on the surface. A linear stability theory reveals a novel mechanism for the excitation of waves. Comparing both the stability diagram and the dispersion relation with experiment, we are able to check the consistency of our model.

83.70.F, 47.54+r, 83.10.Ji

Very little is known about the laws governing the macroscopic motion of granular materials, or for short, “sand”. Most of our information comes from either experiment or microscopic molecular dynamics calculations. An accepted continuum description of sand, analogous to the equations of hydrodynamics, is missing. If such a description exists, it would help our understanding enormously, much in the same way hydrodynamics has dominated our understanding of fluids.

One major difficulty is that sand behaves very differently in different flow situations. If at rest or nearly so, sand behaves like a solid, and the packing of particles is very important [1], while to reach a fluidized state the particles have to be shaken quite violently. Even allowing for flow dependent, non-Newtonian transport coefficients [2], standard hydrodynamic theory hardly accounts for all possible forms of behavior.

Great interest has been stirred by recent experiments in which a thin layer of particles was placed on a plate undergoing sinusoidal vibrations [3–6]. Above a certain vibration amplitude regular and irregular surface-wave patterns were excited subharmonically, i.e. the frequency of the waves is half that of the driving. The observed phenomena are very similar to Faraday waves excited in a periodically vibrated fluid layer. Typical experimental data are the phase diagram of different wave patterns as a function of frequency and acceleration, and the wavelength of the patterns as a function of driving frequency at fixed acceleration. The data turn out to be independent of container size or shape, so the observed patterns represent an intrinsic property of the dynamics of vibrated sand.

The experiments triggered a host of theoretical work in which a wide range of approaches has been used: molecular dynamics calculations [7,8], simplified particle dynamics [9], semi-continuum theories [10,11], phenomenological Ginzburg-Landau models [12], phenomenological coupled map models [13] and order-parameter models

[14]. Most notably, recent molecular dynamics simulations have reproduced the experimental results in great detail [8]. The comparisons between the continuum-type models with experiments have, however, not been very detailed. Their focus was mostly on capturing the localized excitations of the layer (‘oscillons’) that have been observed experimentally [15]. Studies of order-parameter models [16,14] indicate, however, that such localized waves are not specific to granular media and are therefore not the hallmark of these systems.

In the present paper we propose a continuum model for waves in vibrated sand. It is based on the observation that the dispersion relation of the excited waves exhibits a continuum scaling in the small-frequency regime. In this regime an individual grain performs many random collisions, so one can assume correlations between particles to be short-ranged, making a hydrodynamic description feasible. One goal of this investigation is to identify which phenomena do not depend on the granularity, i.e. the discreteness, of the material. Although being akin to a shallow-water theory, the proposed model differs in significant aspects from a fluid-dynamical description. In particular, the unvibrated sand layer exhibits no oscillatory response. In contrast to the Faraday waves in liquids, the excited waves can therefore not be viewed as arising from the resonant driving of damped wave modes of the sand layer.

Central to our model is the experimental observation that the position of the lower rim of the layer of sand is closely modeled by the motion of a single, totally inelastic particle [17]. This is because all the energy is lost upon impact in the inelastic collisions between the grains. The force driving the patterns is thus proportional to the acceleration of the inelastic particle, minus the acceleration of gravity g . At each impact, this relative acceleration $\gamma(t)$ is a δ -function whose strength is the velocity of impact.

We assume that the layer is very thin, so the system is characterized by the thickness and the mean horizontal velocity of the layer alone. For simplicity, we will only consider one-dimensional motion, i.e. stripe patterns. We will not address the nonlinear pattern-selection problem that arises in two-dimensional patterns (e.g. stripes *vs.* squares). From mass and momentum conservation considerations we arrive at equations quite similar to those of a fluid layer in the lubrication approximation, except for some crucial differences to be elaborated below. The equations are

$$h_t + (vh)_x = D_1 h_{xx} \quad (1a)$$

$$h(v_t + vv_x) = -\gamma(t) \frac{h_x}{\sqrt{1+h_x^2}} - Bhv + D_2(v_x h)_x. \quad (1b)$$

Equation (1a) expresses mass conservation, with an Edwards-Wilkinson diffusion term on the right, which describes the tumbling of grains atop one another [18].

Equation (1b) expresses the momentum balance where v is the horizontal velocity integrated over the layer height h . It contains a driving term proportional to both the acceleration $\gamma(t)$ relative to a freely falling reference frame as well as the slope h_x , since particle motion gets started only if the surface is inclined. If we assume that the sand grains are scattered isotropically upon impact and that only those that fly parallel to the surface contribute to the horizontal momentum we obtain the square root in the denominator. We assume that only a surface layer participates appreciably in the flow. Thus, the acceleration term is not proportional to h .

The second and third term on the right describe the friction of the surface layer flowing over the lower layer of sand and the internal (viscous) friction between the flowing particles, respectively. The form of the viscous term ensures a positive definitive energy dissipation [19]. For simplicity, we assume the coefficients of the dissipative terms to be time-independent. In particular, we take the friction force $-Bv$ to be present even if the layer of sand does not rest on the plate. This makes physical sense since the lower portion of the layer is almost at rest relative to the plate. It is only an upper layer which participates in the formation of waves. However, the weight of the whole layer height contributes to the frictional force. To take into account the vertical structure in more detail would require a considerably more sophisticated model [20].

Our model (1) differs from the fluid problem in three ways. First, the driving is nonlinear in h . The square-root in the denominator reflects the assumption that upon impact the sand grains are isotropically dispersed but only those scattered out of the layer contribute to the horizontal flux. Second, in contrast to liquids the sand layer lifts off the plate when the acceleration of the plate exceeds g . Thus, the acceleration term $\gamma(t)$ vanishes over large parts of the cycle and is largest when the sand layer hits the plate. In the following we will assume that it consists mainly of a series of δ -functions. Third, an additional diffusion term appears in the equation for h .

The driving $\gamma(t)$ only depends on the dimensionless acceleration

$$\Gamma = \frac{A\omega^2}{g} \quad (2)$$

of the plate, where A is the amplitude of the harmonic driving with frequency ω . The only other experimental parameters are the filling height h_0 and the grain diameter d . In the following, all quantities will be non-dimensionalized using h_0 as a length scale and $\tau = (h_0/g)^{1/2}$ as a time scale. The dispersion relation

then has the form $q = q(\omega, \Gamma, h_0/d)$. The remarkable observation from the experimental data [17] is that below a cross-over frequency ω_c the dispersion relation is *independent* of h_0/d , i.e. of particle diameter, where h_0/d varies between 3 and 14. This is very reassuring from the viewpoint of continuum theory, where effectively d has been taken to zero. The cross-over frequency ω_c is approximated by the requirement that a particle has enough energy to hop across a neighboring one [17]. Since experiments are performed at constant acceleration, low frequency means large velocities and large kinetic energy. At high frequencies the particles are thus locked into a fixed relative position, which means long-ranged correlations. Only in the fluidized regime $\omega < \omega_c$ is our continuum theory expected to apply.

To understand the instability of the flat layer, we linearize in the variables H and V , with $h = 1 + H$ and $v = V$. The linearized equations of motion can be transformed into a single wave equation for H :

$$H_{tt} = -BH_t + (BD_1 + \gamma)H_{xx} + (D_1 + D_2)H_{txx} - D_1D_2H_{xxxx}. \quad (3)$$

To simplify the analytical calculation we assume that γ consists only of a series of δ -shocks,

$$\gamma(t) = \gamma_0 \sum_{j=-\infty}^{\infty} \delta(t - jT), \quad (4)$$

and neglect the force on the layer during the subsequent time intervals in which the layer is in contact with the plate. With increasing Γ this time interval decreases and for $3.3 < \Gamma < 3.7$ the layer never rests on the plane. Note that γ_0 is the impact velocity, hence it can be written as $\gamma_0 = f(\Gamma)/\omega$.

In between shocks, the solution of (3) is $H \propto e^{\sigma t} e^{iqx}$, where the dispersion relations

$$\sigma_1 = -D_1q^2, \sigma_2 = -B - D_2q^2, \quad (5)$$

correspond to pure relaxation. At the point of impact, the δ -function imposes a jump condition

$$H_t^{(+)} - H_t^{(-)} = \gamma_0 H_{xx}. \quad (6)$$

The height H itself is continuous. By making the general ansatz

$$H_n = \left(\alpha_n e^{\sigma_1(t-nT)} + \beta_n e^{\sigma_2(t-nT)} \right) e^{iqx}$$

and requiring $\alpha_{n+1} = s\alpha_n$ and $\beta_{n+1} = s\beta_n$ for the eigenmode we obtain for the amplification s of the eigenmode

$$s = \pm \left\{ \frac{1}{4} \left[s_1 + s_2 - \gamma_0 q^2 \frac{s_1 - s_2}{\sigma_1 - \sigma_2} \right]^2 - s_1 s_2 \right\}^{1/2} + \frac{1}{2} \left(s_1 + s_2 - \gamma_0 q^2 \frac{s_1 - s_2}{\sigma_1 - \sigma_2} \right), \quad (7)$$

with $s_1 = e^{\sigma_1 T}$ and $s_2 = e^{\sigma_2 T}$. Since $0 < s_1 s_2 < 1$ the condition for instability, $|s| > 1$, can only be satisfied with real $s < -1$. Thus, the only instability is subharmonic, i.e. the motion repeats itself only every other period of the driving, as observed experimentally. Analyzing (7) in the limit $q \rightarrow \infty$ shows that catastrophic instabilities occur if either D_1 or D_2 vanish. This can also be seen directly from (3): Since the driving with γ is proportional to q^2 , only the combined damping $D_1 D_2 q^4$ keeps short-wavelength instabilities at bay. We emphasize that this mechanism for wavenumber selection is quite different from that at work in the fluid case. Faraday waves have the same dispersion relation as if there was no driving, the significance of the driving lies only in exciting the waves. In the case of sand, the medium itself does not support waves as seen from (5); only the interplay of driving and two different kinds of damping selects a wavenumber. Strictly speaking, (5) applies only during the free fall between shocks. Without any periodic forcing a steady component of the vertical acceleration would be present and an oscillatory response of the sand layer would arise in our model unless it is sufficiently damped,

$$B(D_2 - D_1) > 1. \quad (8)$$

Experimentally, however, the layer spends a large fraction of the cycle in free flight already before the onset of waves. Even if (8) should be violated during the brief periods when the layer is in contact with the plate the oscillatory response is not expected to be relevant for the excitation of waves.

Next we compute the most unstable mode on the neutral curve $s = 1$. For supercritical transitions it gives the wavelength that is expected to appear as the acceleration is raised slowly above the critical value γ_{crit} . In the limiting cases $B/\omega \rightarrow \infty$ and $B/\omega \rightarrow 0$ one obtains $q_{crit} \propto (\omega/D_1)^{1/2}$. Since the prefactors differ in the two cases the overall scaling of q_{crit} will, however, in general not be given by $\omega^{1/2}$ as illustrated in Fig.1. We will in fact see below that the dispersion curve is close to linear in the experimentally relevant parameter regime. For large ω the threshold value γ_{crit} becomes independent of ω . With $\gamma_0 \propto f(\Gamma)/\omega$ this implies that for large ω no waves are excited at a given Γ .

A simulation of the full nonlinear model (1) with driving (4) close to the transition confirms the linear stability analysis. The boundary conditions were periodic, and the system size is chosen such that a single wavelength fits into the system at the theoretically known critical wavenumber. The transition turns out to be supercritical, the maximum amplitude of the wave being proportional to $[\gamma_0 - \gamma_0(q_{crit})]^{1/2}$.

We now attempt to make a more quantitative comparison between experimental measurements of the dispersion relation and our model with $\gamma(t)$ now being the full relative acceleration of the sand layer. In the experiment a transition from the flat layer to standing waves is observed at $\Gamma \approx 2.5 - 3$, relatively independent of frequency. We focus on the regime in which continuum

scaling is observed, $\omega < \omega_c \approx 2$. It turns out that in this regime the transition in the experiments is to two-dimensional, square patterns. This does, however, not affect a comparison of the linear properties of the model. The model parameters are determined approximately by requiring that the transition is at $\Gamma \approx 2.5$, independent of frequency. The diffusion constants D_1, D_2 preferentially damp the short wavelength components, while the friction B damps long-wavelength modes. By adjusting the relative strength of either, it is possible to place the maximum growth rate in the right frequency regime, with the onset being just below $\Gamma = 2.5$. This can be achieved for different values of D_2/D_1 . In Fig.2 we show a number of onset curves $\Gamma_{crit}(\omega)$ obtained in this way. Note that the critical wavenumber varies with ω . In the experiments the onset curves remain flat for $\omega > 2$, while in our model Γ_{crit} increases with larger ω . We attribute this difference to the transition to the less fluidized state that occurs around ω_c and beyond which our model is not expected to be applicable.

To find the dispersion relation $q_{crit}(\omega)$ we measure the wavenumber of the fastest growing mode that was obtained when determining the onset curves in Fig.2. The qualitative behavior of the dispersion relation is found to depend only weakly on the ratio D_2/D_1 in this regime. The magnitude of q_{crit} is, however, affected by D_2/D_1 . For $D_1 = 0.6, D_2 = 0.06, B = 0.5$ it compares reasonably well with the experimental results as given in Fig.5.8 in [17]. If a power-law for $q(\omega)$ is assumed the exponent obtained from (1) is, however, lower than found in experiment. Considering the short scaling range available for $\omega < \omega_c$, a power law fit should be viewed with caution. The exponent may easily result from the crossover between two different regimes and is not necessarily an indication of a single physical mechanism behind it. It should be noted that in the experiment the dispersion relation was obtained by measuring the wave number of the patterns that were obtained when ω was scanned at a fixed value of $\Gamma = 2.5$ above onset. Above onset a whole range of wave numbers is accessible and the resulting wave number depends on the nonlinear evolution of the pattern from the initial conditions (random in the experiment); in principle, it need not be the wave number of the mode with the largest linear growth rate [21].

It is expected that better agreement can be obtained if additional aspects of the system are included in the model. For instance, we have neglected effects of a layer dilation, which will depend on frequency; a dilated layer will have a lower density, while we assumed the density to be constant. In addition, the dilation will smooth out the δ -driving, making the driving less effective, and lowering γ_0 . For the same reasons, there could be an effective dependence of the viscous parameters D_1, D_2 , and B on the frequency. Such a dependence of the force necessary to drag a sphere through a layer of vibrated sand was found in [22]. In addition, only a certain part of the layer takes part in the horizontal motion. In [11] this was accounted for by introducing a ‘‘penetration depth’’, which is an un-

known function of parameters. This was crucial for obtaining a transition between a high and a low frequency regime. Within the approach followed here an effective frequency-dependence of coefficients would be obtained more appropriately by introducing additional dynamical degrees of freedom as, for instance, the dilation of the granular layer. Here we stick to the results obtainable without such complications.

Turning to the nonlinear behavior of the model, we find that the bifurcation is supercritical (as in the similar model proposed in [11]), while experimentally the transition is subcritical [4,5]. We investigate possible mechanisms for a subcritical transition. The subcritical nature of the transition is important for the appearance of localized excitations of the flat state, called oscillons [15]. When the layer is hardly in motion, the stick friction between particles in contact will produce a much higher effective viscosity than if the layer was fluidized. We model this effect by allowing D_2 to depend on the local velocity:

$$D_2 = D_2^{(0)} \left[1 + \eta e^{-(v/v_0)^2} \right]. \quad (9)$$

Using $\eta = 0.5$ and $v_0 = 0.2$ as parameters, we now find a hysteretic transition as shown in Fig.4. This is no surprise, because the motion has to work against a higher effective viscosity when it starts from rest.

So far we have seen no evidence for oscillons in our one-dimensional model even with a fairly strong hysteresis. One explanation is that the sharp peak characteristic for oscillons results from the focusing of grains as they move radially inward. We plan to account for this effect by constructing a radially symmetric code, with the oscillon at the coordinate center.

In conclusion, we have presented a continuum model for the parametric excitation of surface waves in granular media. It takes into account the extremely strong damping in these systems, i.e. the absence of any damped wave modes, and the specific form of the driving through shock-like impacts that are due to the lift-off of the granular medium. The dispersion relation of this model compares favorably with experimental data. In its simplest form the model does not reproduce the hysteresis observed in the experiments. It therefore requires the introduction of additional features like a threshold in the slope of the surface for the excitation of waves, which might mimic an effect akin to an angle of repose. Keeping with the spirit of the continuum model, which to some extents assumes the material to be fluidized, we introduced instead a dependence of the dissipation on the velocity, which models the varying degree of fluidization of the material.

The authors thank H.L. Swinney and P.B. Umbanhowar for sharing their experimental data prior to publication. HR gratefully acknowledges instructive discussions with T. Shinbrot. This work was supported by the United States Department of Energy through grant

DE-FG02-92ER14303 and by the Deutsche Forschungsgemeinschaft through SFB 237.

-
- [1] H. Jaeger and S. Nagel, *Science* **255**, 1523 (1992).
 - [2] S. Savage, R. Neddermann, U. Tüzün, and G. Houlsby, *Chem. Eng. Sci.* **38**, 189 (1983).
 - [3] S. Douady, S. Fauve, and C. Laroche, *Europhys. Lett.* **8**, 621 (1989).
 - [4] F. Melo, P. Umbanhowar, and H. Swinney, *Phys. Rev. Lett.* **72**, 172 (1994).
 - [5] F. Melo, P. Umbanhowar, and H. Swinney, *Phys. Rev. Lett.* **75**, 3838 (1995).
 - [6] R. Metcalf, J. Knight, and H. Jaeger, *Physica A* **236**, 202 (1997).
 - [7] K. Aoki and T. Akiyama, *Phys. Rev. Lett.* **77**, 4166 (1996).
 - [8] C. Bizon *et al.*, *Phys. Rev. Lett.* **80**, 57 (1998).
 - [9] T. Shinbrot, *Nature* **389**, 574 (1997).
 - [10] D. Rothman, *Phys. Rev. E* **57**, 1239 (1998).
 - [11] E. Cerda, F. Melo, and S. Rica, *Phys. Rev. Lett.* **79**, 4570 (1997).
 - [12] L. Tsimring and I. Aranson, *Phys. Rev. Lett.* **79**, 213 (1997).
 - [13] S. Venkataramani and E. Ott, *Phys. Rev. Lett.* **80**, 3495 (1998).
 - [14] C. Crawford and H. Riecke, *Physica D* (submitted).
 - [15] P. Umbanhowar, F. Melo, and H. Swinney, *Nature* **382**, 793 (1996).
 - [16] H. Sakaguchi and H. Brand, *Europhys. Lett.* **38**, 341 (1997).
 - [17] P. Umbanhowar, Ph.D. thesis, U. Texas, Austin, 1996.
 - [18] S. Edwards and D. Wilkinson, *Proc. R. Soc. Lond. A* **381**, 17 (1982).
 - [19] J. Eggers and T. Dupont, *J. Fluid Mech.* **262**, 205 (1994).
 - [20] To obtain $h(v_t + vv_x)$ in (1b) from the material derivative $D(hv)/Dt$ mass conservation (1a) is used. However, the diffusion term $D_1 h_{xx}$, which would lead to an additional, nonlinear term in the momentum equation, comes from grains flying above the layer. This requires a much more sophisticated model to be treated consistently, and is therefore ignored in the following.
 - [21] H. R. Schöber, E. Allroth, K. Schröder, and H. Müller-Krumbhaar, *Phys. Rev. A* **33**, 567 (1986).
 - [22] O. Zik, J. Stavans, and Y. Rabin, *Europhys. Lett.* **17**, 315 (1992).

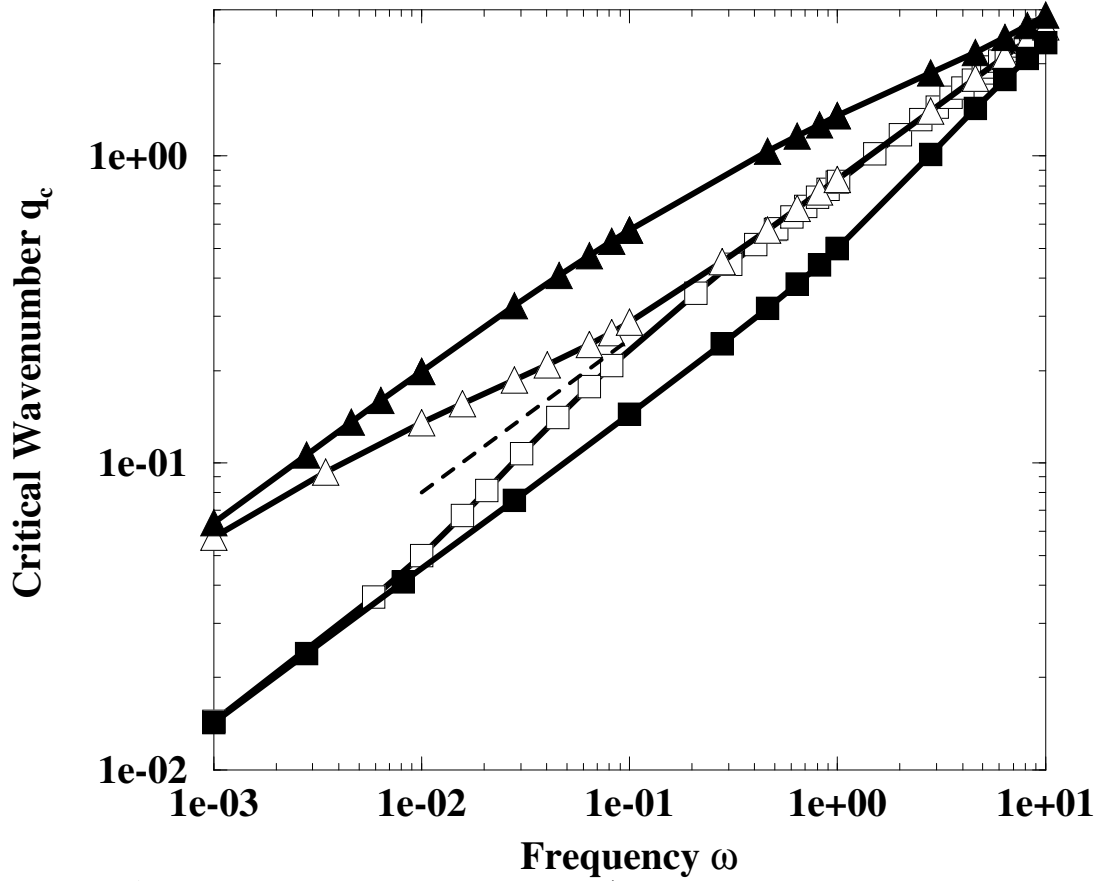


FIG. 1. Analytical dispersion relation for $B = 0.01$ (open symbols) and $B = 1$ (filled symbols) for $D_1 = 1$ and $D_2 = 0.05$ (squares) and for $D_1 = 0.05$ and $D_2 = 1$ (triangles). The dashed line indicates square-root behavior.

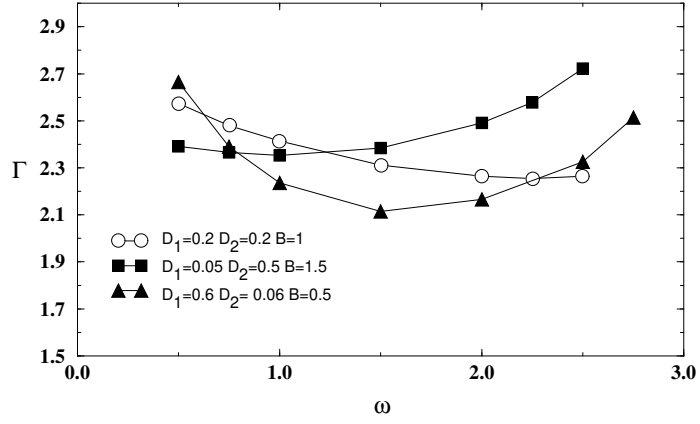


FIG. 2. Neutral curves $\Gamma_{crit}(\omega)$ for different combinations of the dissipative parameters D_1 , D_2 and B (open circles $D_1 = D_2 = 0.2$, $B = 1$, solid squares $D_1 = 0.05$, $D_2 = 0.5$, $B = 1.5$, solid triangles $D_1 = 0.6$, $D_2 = 0.06$, $B = 0.5$)

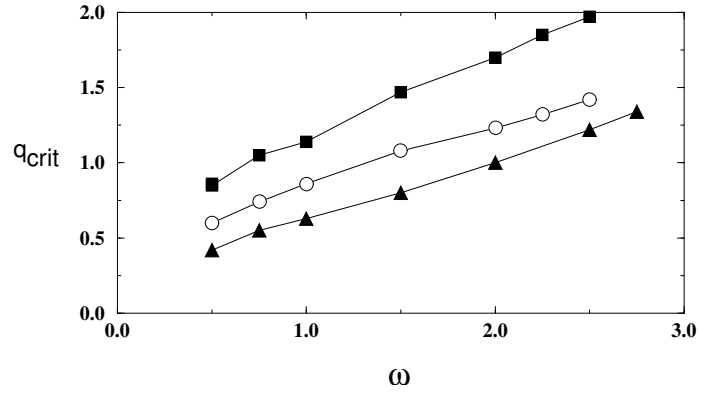


FIG. 3. Dispersion relation $q_{crit}(\omega)$ corresponding to the neutral curves in Fig.2.

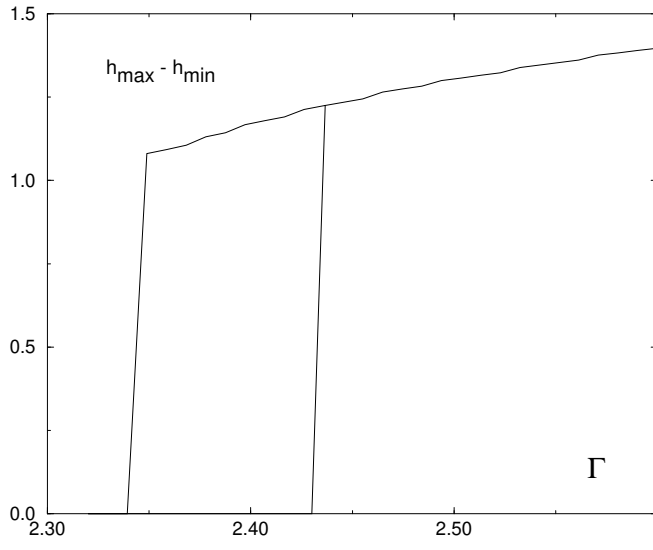


FIG. 4. Hysteretic nature of the transition in the presence of a velocity-dependent viscosity (9) with $\eta = 0.5$ and $v_0 = 0.2$.